The pseudo-spectral code MagIC/PaRoDy

L.Petitdemange &R.Raynaud

Observatoire de Paris, Département d'Astrophysique du CEA-Saclay

Atelier Codes AIPS/PNPS
Meudon, June 29th, 2022

Laboratoire d'Étude du Rayonnement et de la Matière en Astrophysique

Programme National de Physique Stellaire

Table of contents

MagIC overview

What for ?

- fluid dynamics a in a rotating spherical shell
- solve for the coupled evolution of
  1. sound-proof approximations of the Navier-Stokes equation
  2. heat transfer equation
  3. chemical composition equation
  4. induction equation
- mixed implicit/explicit time step scheme
- hybrid OpenMP/MPI parallelisation,
  scales up to 1000 processors

Applications: from geophysics to stellar physics

Geodynamo models

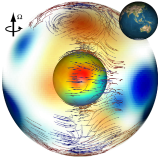

Aubert, 2008

Rayleigh-Bénard convection

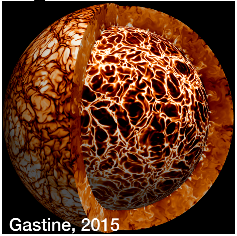

Gastine, 2015

Spherical Couette dynamo

Cao, 2012

Jupiter: zonal jets, dynamo

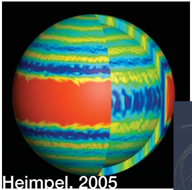

Heimpel, 2005

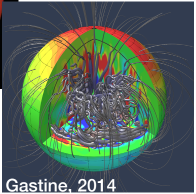

Gastine, 2014

Stellar physics

MRI in a spherical shell

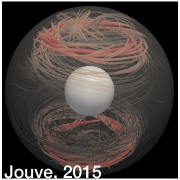

Jouve, 2015

Formation of polar spots in fully convective stars

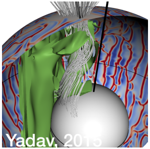

Yadav, 2015

Table of contents

Rotation effects in spherical Couette flow

Axisymmetric models can be used as $Re \ll 1$ and $Ro \ll 1$.
The Ekman number
$E = \frac{\text{viscous}}{\text{Coriolis}} = \frac{\nu}{\Omega L^2}$.
In stellar interiors $E \sim 10^{-15}$.

Dormy *PhD thesis* (1998)

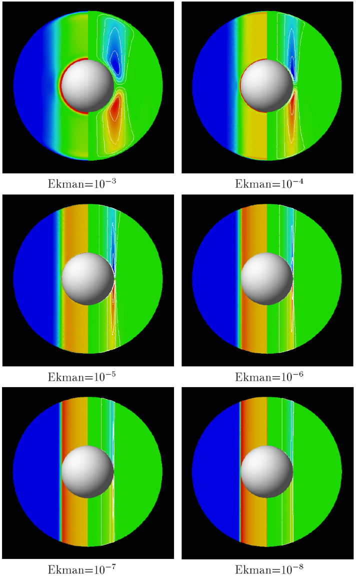

Magnetic effects in rapidly rotating Spherical Couette Flow ($\mathbf{B} = Bz$)

Rapidly rotating systems

Geostrophic balance

$$2\Omega \mathbf{e_z} \times \mathbf{u} = -\nabla\pi$$

Proudman-Taylor Theorem:

$$\frac{\partial \mathbf{u}}{\partial z} = \mathbf{0}$$

Magnetostrophic balance

$$2\Omega \mathbf{e_z} \times \mathbf{u} = -\nabla\pi + \frac{1}{\mu_0\rho_0}(\nabla \times \mathbf{B}) \times \mathbf{B}$$

$$R_o = \frac{\Delta\Omega}{\Omega} \ll 1$$

Angular velocity

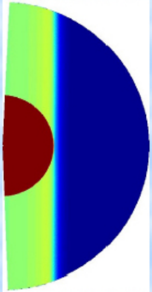

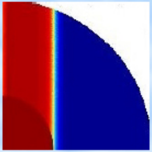

MHD stationnary solution with only vertical B field

A super-rotating shear layer induced by a strong dipolar field

The Elsasser number: $\Lambda = \dfrac{B_0^2}{\mu_0 \rho_0 \Omega_0 \eta}$

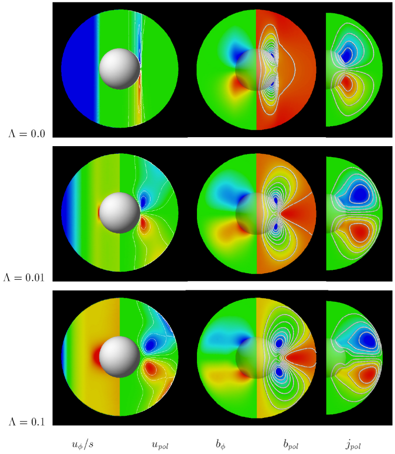

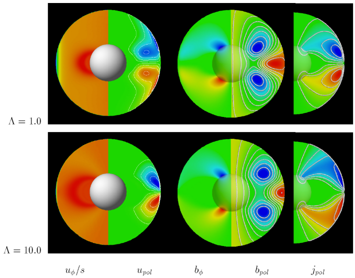

Parameter study (Dormy *et al* 1998)

Rotation influence on the magnitude of the super-rotating shear layer

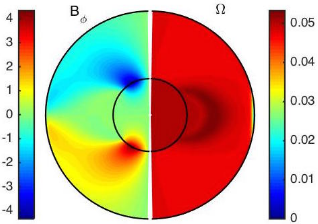

$E = 10^{-5}$, $\Lambda = 1$

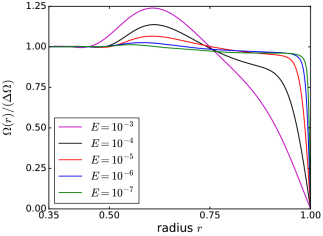

$\Lambda = 1$

The magnitude of the super-rotating layer decreases as the global rotation increases ($E \to 0$)

Stably-Stratification affects the geometry of the angular velocity

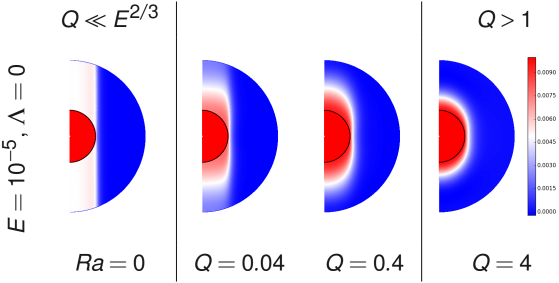

$Q = Pr\left(\frac{N}{\Omega_0}\right)^2 = E^2 Ra$ where N: Buoyancy frequency

A super-rotating shear layer in strongly magnetized radiative zones

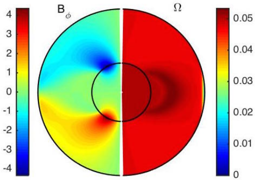

$E = 10^{-5}$, $Ra = 0$, $\Lambda = 1$

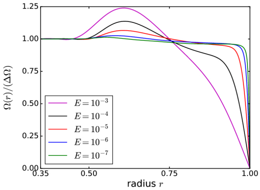

$\Lambda = 1$, $Ra = 0$

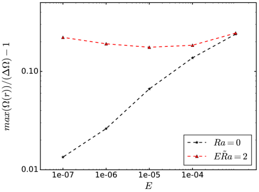

$\Lambda = 1$ $Q \sim 1$

Stratification enables to maintain the super-rotating shear layer for lower Ekman numbers

(Philidet, Gissinger, Lignières, Petitdemange (2019) *GAFD*)

Lignes directrices

One example with PaRoDy: DNS of the Tayler-Spruit instability

Florentin Daniel **Ludovic Petitdemange** **Florence Marcotte**
Christophe Gissinger

LPENS/LERMA
Workshop Codes and Stellar Physics

June 29th 2022

Table of contents

Table of contents

Context

Angular momentum in the radiative zone of stars

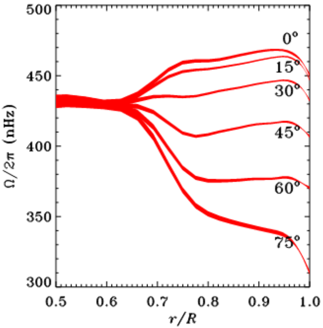

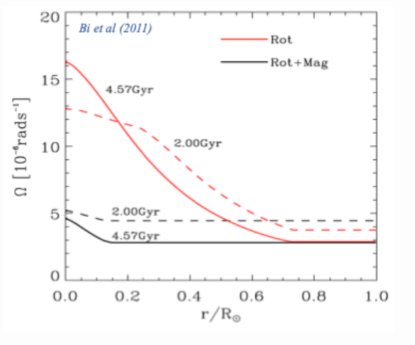

Figure 1 – Left : Rotation profile at constant latitude in the sun (Brown et al. 1989). Right : Numerical simulation for the radiative zone of a star, with and without magnetic field.

Table of contents

Spruit 2002

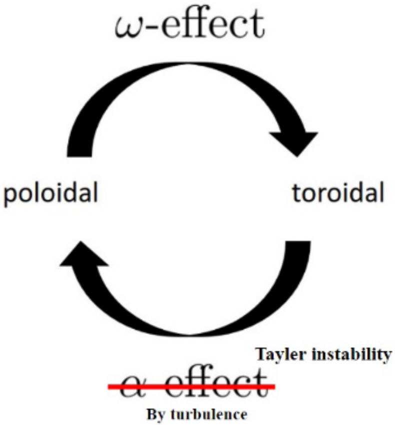

Figure 2 – Spruit's dynamo loop

Spruit 2002

Instability conditions (Spruit 1999)

$$s\frac{d}{ds}\left(\frac{V_A^2}{s^2}\right) > 0 \text{ for } m = 0 \tag{1}$$

$$\frac{1}{s^3}\frac{d}{ds}\left(s^2 V_A^2\right) > \frac{m^2 V_A^2}{s^2} \text{ for } m > 0 \tag{2}$$

The $m = 1$ modes require less steep variations of $V_A = B_\phi/\sqrt{\mu\rho}$.
Cylindrical coordinates (s, ϕ, z).
Rotation, diffusion and stratification are known to have a stabilizing influence on Tayler's modes. Using simplications and heuristic arguments :

$$\frac{\omega_{A0}}{\Omega} > \left(\frac{N}{\Omega}\right)^{1/2}\left(\frac{\eta}{r^2\Omega}\right)^{1/4} \quad \kappa = 0 \tag{3}$$

$$\frac{\omega_{A1}}{\Omega} > \left(\frac{N}{\Omega}\right)^{1/2}\left(\frac{\kappa}{r^2\Omega}\right)^{1/4}\left(\frac{\eta}{\kappa}\right)^{1/2} \quad \omega_A = \frac{V_A}{S} \tag{4}$$

Table of contents

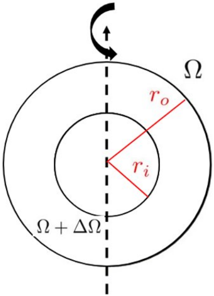

$\mathbf{u}, \mathbf{B}, \Theta$?

$$\chi = \frac{r_i}{r_o} = 0.35$$

$$\nu, \kappa, \eta$$

$$\Delta T$$

Figure 3 – Geometry

- No slip on both boundaries
- Initial magnetic field arbitrary weak
- Imposed inner rotation
- Boussinesq

Equations

$$\frac{\partial \mathbf{u}}{\partial t} + (\mathbf{u}.\nabla)\mathbf{u} = -\nabla P - 2\frac{1}{ER_e}\mathbf{e_z} \times \mathbf{u} + \frac{1}{R_e}\Delta \mathbf{u} + \left(\frac{1}{ER_e} + \frac{1}{\chi}\right)(\nabla \times \mathbf{B}) \times \mathbf{B} \quad (5)$$

$$+ \frac{R_a}{P_r R_e^2}\Theta \mathbf{e_r} \quad (6)$$

$$\nabla.\mathbf{u} = 0 \quad (7)$$

$$\frac{\partial \Theta}{\partial t} + (\mathbf{u}.\nabla)\Theta = \frac{1}{P_r R_e}\Delta\Theta - (\mathbf{u}.\nabla)T_s \quad (8)$$

$$\frac{\partial \mathbf{B}}{\partial t} = \nabla \times (\mathbf{u} \times \mathbf{B}) + \frac{1}{P_m R_e}\Delta \mathbf{B} \quad (9)$$

$$\nabla.\mathbf{B} = 0 \quad (10)$$

$$R_e = \frac{r_o r_i \Delta\Omega}{\nu}, E = \frac{\nu}{r_o^2 \Omega}, R_a = \frac{\alpha \Delta T g r_o^3}{\nu\kappa}, P_r = \frac{\nu}{\kappa}, P_m = \frac{\nu}{\eta} \quad (11)$$

Code

- Typical resolution $[N_r \times N_\theta \times N_\phi] = [336, 240, 192]$
- Time of integration : t_ν, t_η

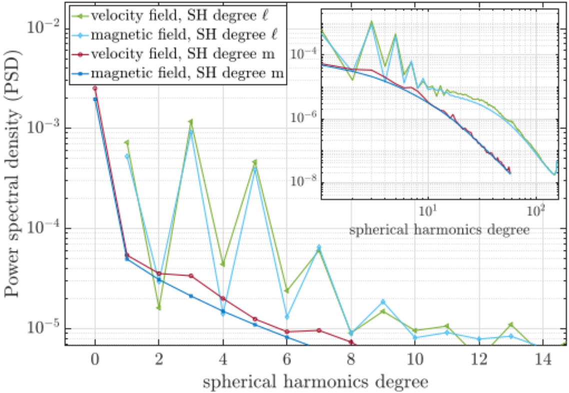

Figure 4 – Power spectra of the velocity and magnetic fields of the first spherical harmonic degrees *m* and *l*. *Inset* : same, showing now the full spectra. Parameters : $E = 10^5$, $R_e = 2, 75.10^4$, $P_m = 1$, $P_r = 0.1$ and $R_a = 10^9$.

Table of contents

Results

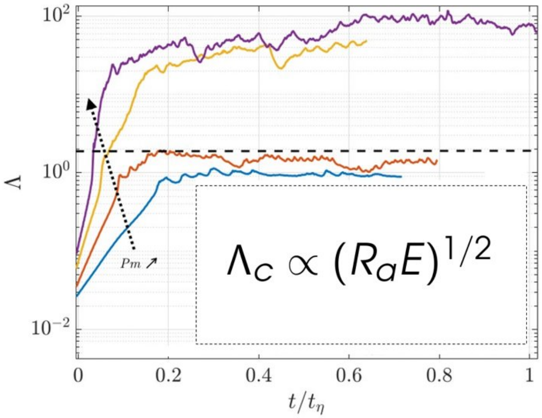

Figure 5 – Timeseries of the magnetic energy (measured by the Elsasser number Λ) for $E = 10^5$, $R_a = 10^9$, $P_r = 0.1$, $Re = 27500$ and varying magnetic Prandtl number $Pm = [0.35; 0.42; 0.5; 1]$, in resistive timescale. *Inset :* Threshold for Tayler instability

Results

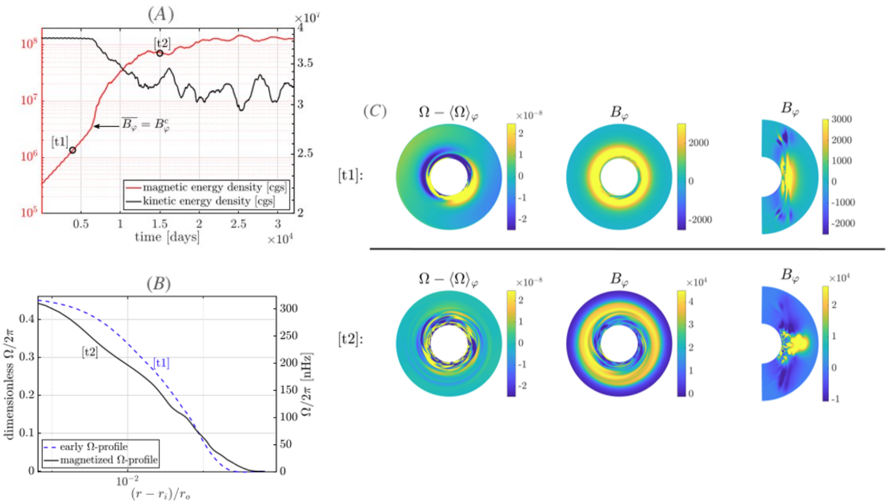

Figure 6 – (A) : Timeseries of the total kinetic and magnetic energies, and radial profiles of the azimuthally-averaged angular velocity in the equatorial plane (B) for two distinct times, marked as (t1) and (t2) in the timeseries. (C) Equatorial cuts

Subcritical transition to turbulence

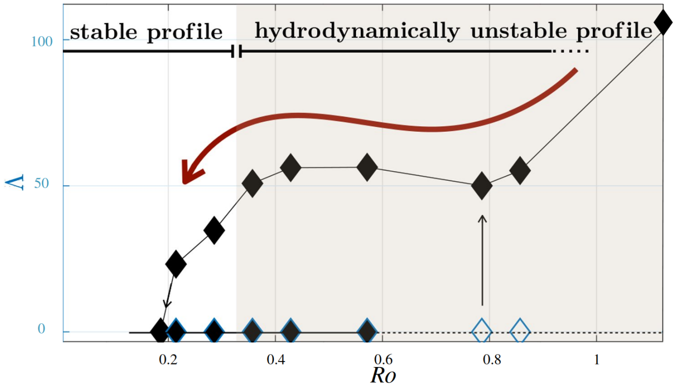

Figure 7 – Time-averaged magnetic energy density of the saturated dynamo versus shear rate (Rossby number $R_o = ER_e$), for $E = 10^5$, $R_a = 10^9$, $P_r = 0.1$ and $P_m = 1$.

Table of contents

Transport

- Angular Momentum
- Turbulent diffusion coefficients

Torques

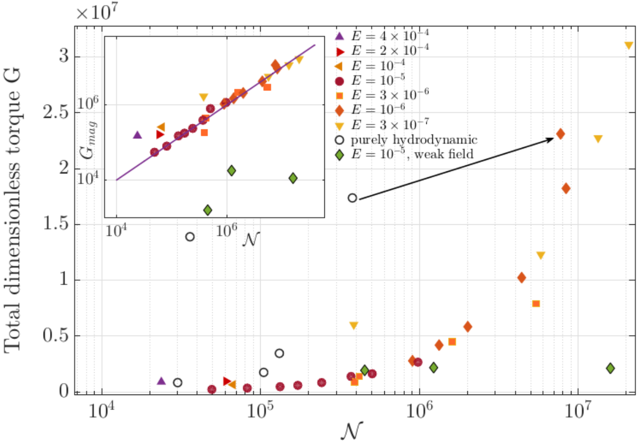

Figure 8 – Total dimensionless torque G exerted on the inner sphere as a function of Spruit's dimensionless quantity $\mathcal{N} = Ar_i^{5/2} \frac{(U_0\Omega)^{3/2}}{N\nu^2}$. *Inset :* Magnetic torque only, shown here for a wide range of parameters values and compared to Spruit's theoretical prediction. The arrow compares two simulations with identical control parameters, with and without magnetic fields.

Conclusion

- Tayler-Spruit (TS) dynamo seems to be now supported by Direct Numerical Simulations.
- Subcritical behaviour : hidden magnetic fields trigger MHD turbulence that transport angular momentum.
- Stratification enables the development of TS dynamos in DNS.
- In progress :
  - Exploring different parameter regimes.
  - Determining the transport coefficients and the dynamo properties.
  - Considering a more realistic model for the radiative zone.
  - Link with observations. . .

κ_T/κ via Nussel thermique

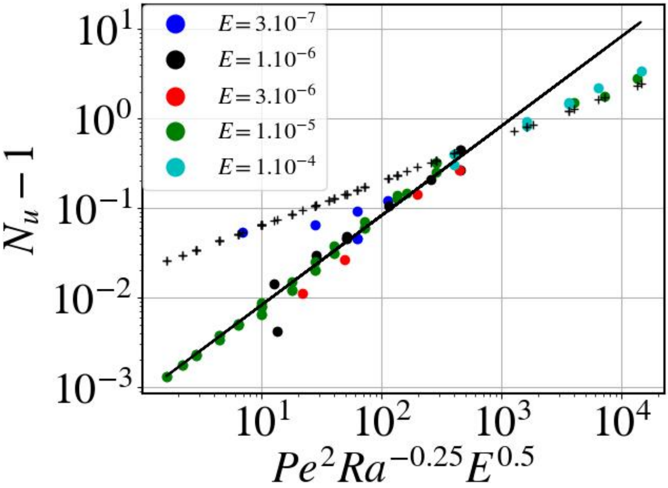

Lignes directrices

1. Introduction
2. **Science with *PaRoDy* or MagIC**
   - 3D MHD Spherical Couette Flow: Tayler-Spruit dynamo
   - **MRI in rapidly rotating spherical shells**
   - Convective dynamos
   - Coriolis effects in hydro anelastic models
   - Magnetic effects
3. Numerical methods
   - The poloidal/toroidal decomposition
   - Angular decomposition: Spherical Harmonics (SH)
   - Rdial discretization
   - Time integration
   - Resolution cheks

Natural candidate for the MRI Accretion Disks

Planet and Stellar Formation

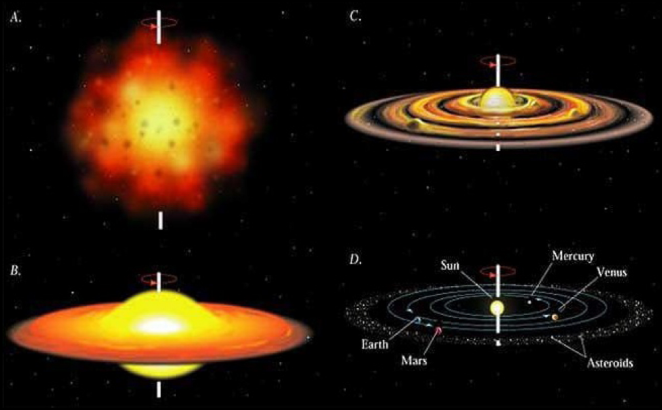

MRI triggers turbulence and allows accretion

Instability mechanism

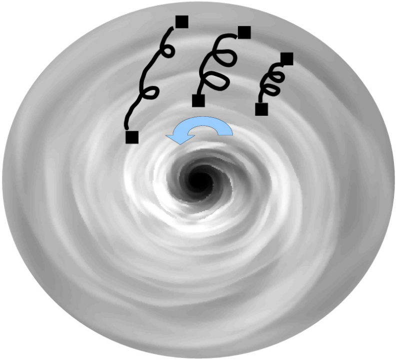

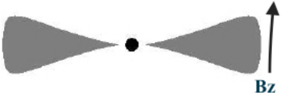

Keplerian rotation rate

$$\Omega^2 = \frac{GM}{R^3}$$

Unstable MRI modes in rapidly rotating systems

MRI takes a particular structure when the Coriolis force dominates

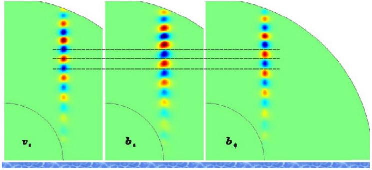

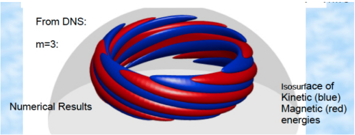

Petitdemange *et al* (2008) *GRL* ; Petitdemange *et al* (2013) *PEPI*

With an applied velocity field

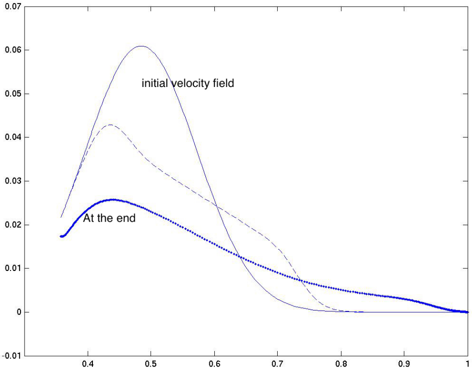

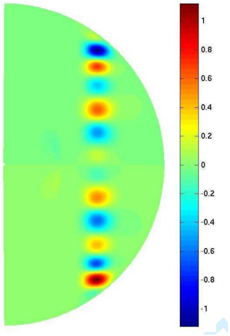

At the end: $Ro' = \frac{d \ln \Omega}{d \ln s} = 0.0062$

With an applied velocity field

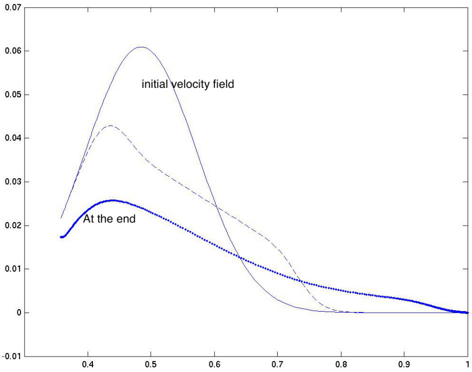

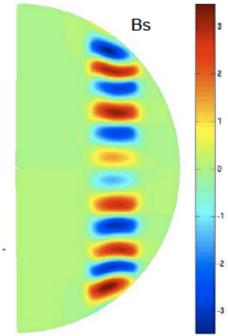

At the end: $Ro' = 0.0062$.

Time evolution of the shear rate

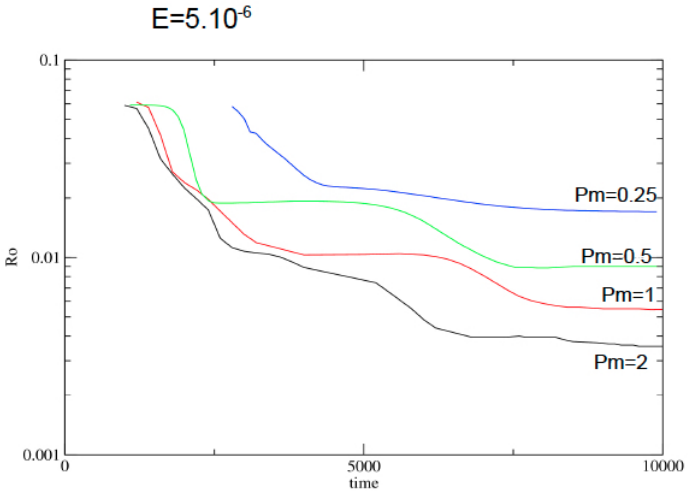

Lignes directrices

Convection in rotating spherical shells

Vorticity
$$\omega_z = (\nabla \times \mathbf{v}) \cdot \mathbf{e}_z$$

Equatorial cuts

Azimuthal sections

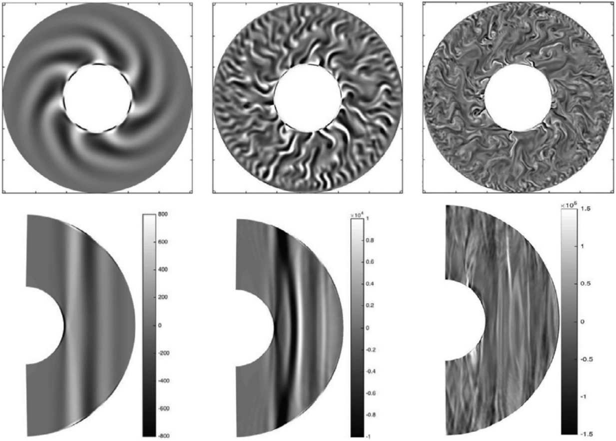

$Ra = 3Ra_c$ $\quad Ra = 10Ra_c$ $\quad Ra = 50Ra_c$.

Petitdemange *PEPI* 2018

Earth's magnetic field: dipole-dominated dynamo

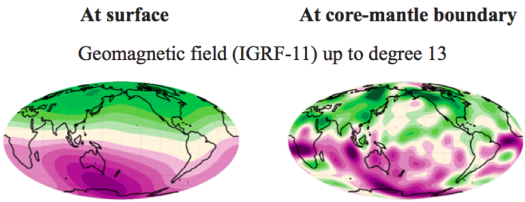

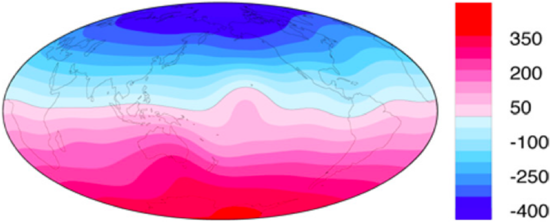

Time-averaged CMB field over 0–0.5 Myr from lava and sedimentary data (Johnson and Constable 1997). This material is adapted from Johnson *et al* (2008) with permission from John Wiley & Sons, Inc. Copyright 2008.

geodynamo simulations

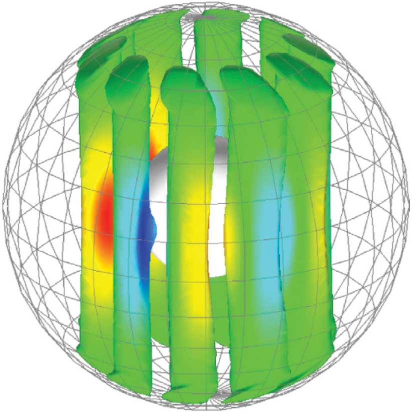

Dormy *et al* 2004

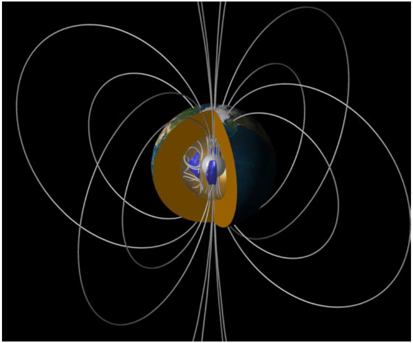

Aubert HDR

Geodynamo simulations

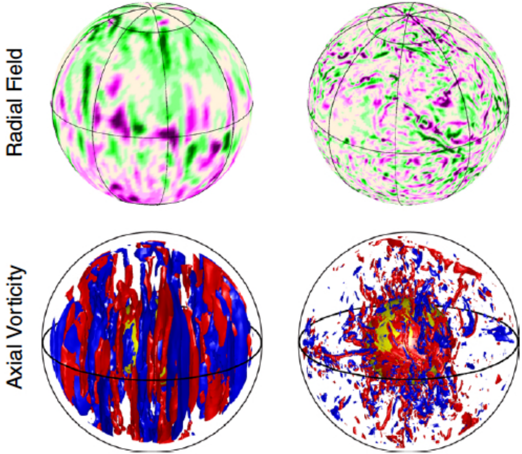

Soderlund *et al* 2012

Snapshots

$N_\rho = 1.5, Pm = 0.75, Ra/Ra_c = 5$ | $N_\rho = 2.5, Pm = 2, Ra/Ra_c = 3.4$

$B_r(r = r_o)$

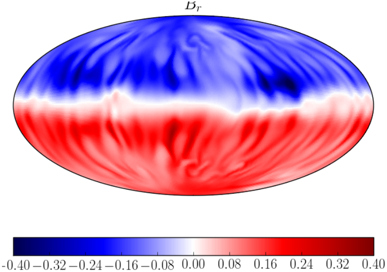

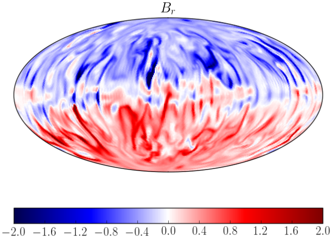

V_r

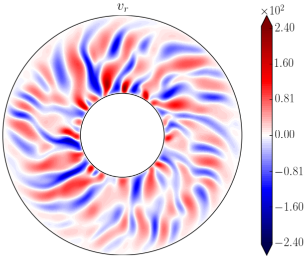

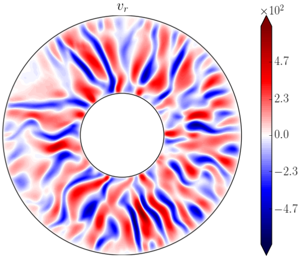

Bistability

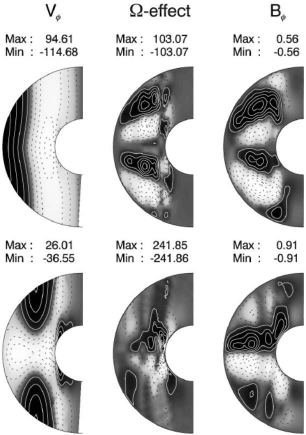

Bistability
SF/SF B.C.

multipolar field branch

Oscillatory dynamos

Dipolar field branch

Dipolar and stationary

Schrinner, Petitdemange, Dormy (2012) Ap.

Dynamo regimes in Boussinesq and Anelastic models

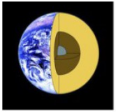

From geodynamo to solar magnetism

Magnetic field topology in
in direct numerical simulations

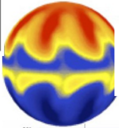

Dipole collapse when the aspect ratio
is higher than 0.65 as the size
of convective cells increases $Ro_\ell > 0.1$

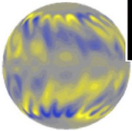

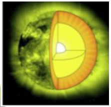

Results obtained in Boussinesq $\rho=\rho_0$ and anelastic :

$$N_\rho = \ln\left(\frac{\rho(r=r_i)}{\rho(r=r_o)}\right)$$

$$\vec{\nabla}\cdot(\rho(r)\vec{v}) = 0$$

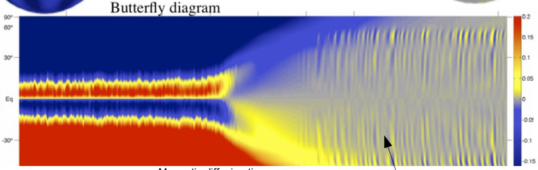

Local Rossby

$$Ro_\ell = Ro\frac{L}{\ell_c} = \frac{u_{rms}}{\Omega L}\frac{L}{\ell_c}$$

ℓ_c : size of convection cells

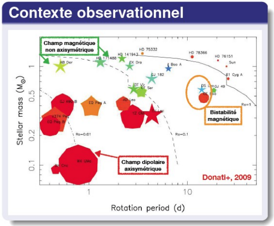

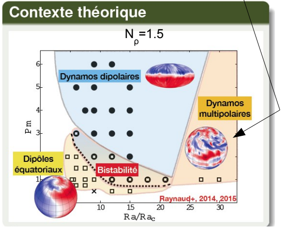

Systematic parameter studies allow to deduce the influences of the physical ingredients as the differential rotation which plays a major role in oscillatory dynamos.

Schrinner et al (2012), ApJ.
Schrinner et al (2014) A&A
Raynaud et al (2014) A&A
Raynaud et al (2015) MNRAS
Petitdemange (2018) PEPI
Raynaud et al (2018) A&A

Lignes directrices

Convection in compressible systems

Anti-correlation between the heat-flux measured by the Nusselt number *Nu* (black) and V_ϕ. (blue)

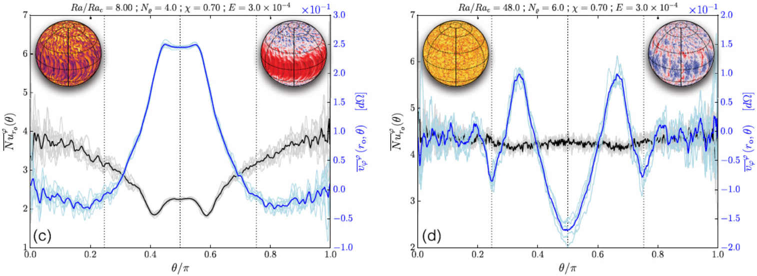

$N_\rho = 4$, $\rho_i/\rho_o = 54$ $N_\rho = 6$, $\rho_i/\rho_o = 400$.

Raynaud, Rieutord, Petitdemange, Gastine, Putigny, (2018) *A&A*

Entropy, Velocity magnitude and Nusselt number snapshots

$N_\rho = 2$ $N_\rho = 6$

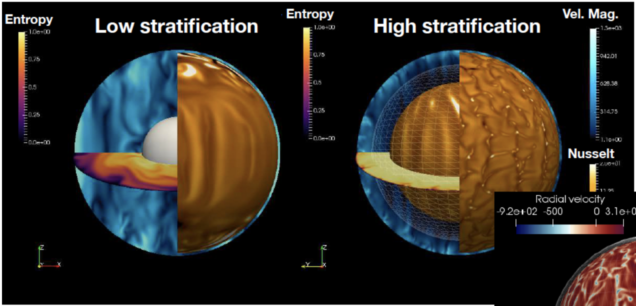

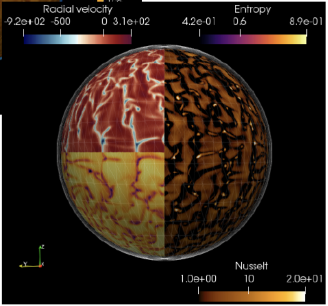

$N_\rho = 8$, $\rho_i/\rho_o = 3000$

Coriolis effect: a parameter study

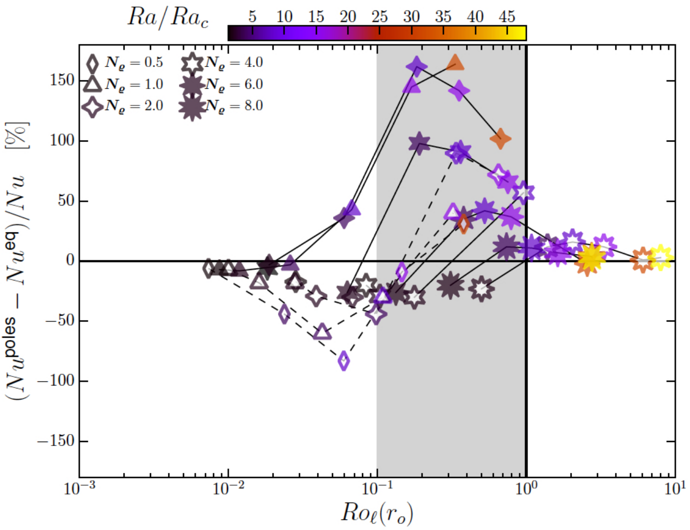

Lignes directrices

What about MHD effects? Hemispherical oscillatory dynamos

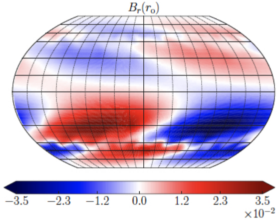

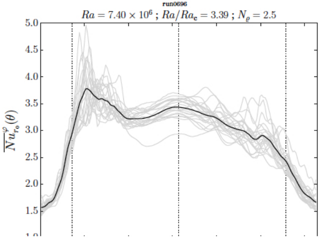

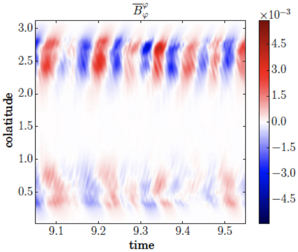

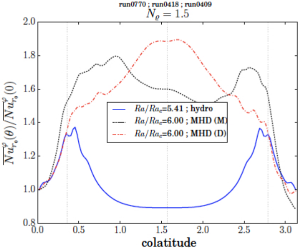

Uniformisation of the heat flux distribution by magnetic fields

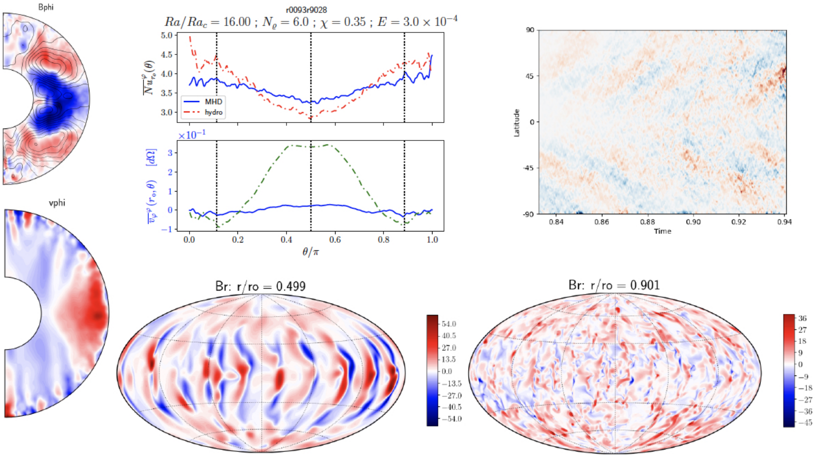

Table of contents

PaRoDy and MagIC: in words

- They simulate rotating fluid dynamics in a spherical shell
- They solve for the coupled evolution of Navier-Stokes, magnetic and temperature (or entropy) equations and an equation for chemical composition under both the anelastic and the Boussinesq approximations.
- A dimensionless formulation of the equations is assumed
- MagIC is a free software (GPL), they are written in Fortran.
- Post-processing relies on python libraries (MagIC)
- Poloidal/toroidal decomposition is employed.
- They use spherical harmonic decomposition in the angular directions
- Finite differences (or Chebyshev polynomials for MagIC) are employed for the radial discretisation.
- They use a mixed implicit/explicit time stepping scheme.
- They relie on a hybrid parallelisation scheme (MPI/OpenMP).

Lignes directrices

The poloidal/toroidal decomposition of soleonidal vectors

PaRoDy

$$\mathbf{v} = \nabla\times\nabla\times(\mathbf{r}v_P) + \nabla\times(\mathbf{r}v_T)$$

$$\mathbf{v} = \begin{array}{l} \frac{1}{r}L_2 v_P \mathbf{e}_r \\ \left(\frac{\partial}{\partial\theta}\left(\frac{1}{r}\frac{\partial}{\partial r}(rv_P)\right) + \frac{1}{\sin\theta}\frac{\partial v_T}{\partial\phi}\right)\mathbf{e}_\theta \\ \frac{1}{\sin\theta}\left(\frac{\partial}{\partial\phi}\left(\frac{1}{r}\frac{\partial}{\partial r}(rv_P)\right) - \frac{\partial v_T}{\partial\theta}\right)\mathbf{e}_\phi \end{array}$$

$$\nabla\cdot\mathbf{v} = 0 \Leftrightarrow \quad \mathbf{v} = \mathbf{P} + \mathbf{T}$$

$$\mathbf{v} = \nabla\times\nabla\times(W\mathbf{e_r}) + \nabla\times(Z\mathbf{e_r})$$

$$\nabla\cdot(\bar{\rho}\mathbf{v}) = 0 \Leftrightarrow \quad \bar{\rho}\mathbf{v} = \mathbf{P} + \mathbf{T}$$

$$\bar{\rho}\mathbf{v} = \nabla\times\nabla\times(W\mathbf{e_r}) + \nabla\times(Z\mathbf{e_r})$$

W is the poloidal potential and Z is the toroidal potential (MagIC).

A useful decomposition

- It enables to ensure the divergence-free conditions.
- v_r is purely poloidal and v_ϕ (m=0) is purely toroidal.
- 3 unknowns of a solenoidal vector replaced by 2 scalar fields.

The toroidal/poloidal decomposition

$$\mathbf{v} = \nabla \times \nabla \times (\mathbf{r} v_P) + \nabla \times (\mathbf{r} v_T) \quad (1)$$

$$\mathbf{v} = \begin{aligned} & \frac{1}{r} L_2 v_P \mathbf{e}_r & (2) \\ & \left(\frac{\partial}{\partial \theta} \left(\frac{1}{r} \frac{\partial}{\partial r} (r v_P) \right) + \frac{1}{\sin\theta} \frac{\partial v_T}{\partial \phi} \right) \mathbf{e}_\theta & (3) \\ & \frac{1}{\sin\theta} \left(\frac{\partial}{\partial \phi} \left(\frac{1}{r} \frac{\partial}{\partial r} (r v_P) \right) - \frac{\partial v_T}{\partial \theta} \right) \mathbf{e}_\phi & (4) \end{aligned}$$

where L_2 is the operator:

$$L_2 = -r^2 \Delta_H = -\frac{1}{\sin\theta} \frac{\partial}{\partial \theta} \left(\sin\theta \frac{\partial}{\partial \theta} \right) - \frac{1}{\sin\theta} \frac{\partial^2}{\partial \phi^2} \quad (5)$$

Useful mathematical identities

- Solenoidal fields $\implies$ poloidal/toroidal decomposition

$$\nabla\cdot\mathbf{B}=0 \iff \mathbf{B}=\boldsymbol{\nabla}\times\boldsymbol{\nabla}\times B_P\mathbf{e}_r+\boldsymbol{\nabla}\times B_T\mathbf{e}_r$$

$$\mathbf{e}_r\cdot\mathbf{B}=-\Delta_H B_P \qquad ; \qquad \mathbf{e}_r\cdot(\nabla\times\mathbf{B})=-\Delta_H B_T$$

$$\nabla\times\mathbf{B}=-\nabla\times(\mathbf{r}\Delta B_P)+\nabla\times\nabla\times(\mathbf{r}B_T)$$

$$\nabla\times\nabla\times\mathbf{B}=-\nabla\times\nabla\times(\mathbf{r}\Delta B_P)-\nabla\times(\mathbf{r}\Delta B_T)$$

- Spherical harmonic decomposition in the angular directions

$$F(r,\theta,\varphi)=\sum_{l=0}^{+\infty}\sum_{m=0}^{l} f_l^m(r)\,Y_l^m(\theta,\varphi)+\text{c. c.}$$

$$\Delta_H Y_l^m = l(l+1)/r^2\,Y_l^m \quad L_2\,Y_l^m = l(l+1)\,Y_l^m$$

Using notations as in MagIC manual

From vectorial to toroidal and poloidal equations via operators:

$$\mathbf{e_r} \cdot [\tilde{\rho}\mathbf{v}] = -\Delta_H W$$
$$\mathbf{e_r} \cdot [\nabla \times \tilde{\rho}\mathbf{v}] = -\Delta_H Z$$

where Δ_H denotes the horizontal part of the Laplacian:

$$\Delta_H = \Delta - \frac{1}{r^2}\frac{\partial}{\partial r}\left(r^2\frac{\partial}{\partial r}\right) = \frac{1}{r^2 \sin\theta}\frac{\partial}{\partial\theta}\sin\theta\frac{\partial}{\partial\theta} + \frac{1}{r^2\sin\theta}\frac{\partial^2}{\partial^2\phi}$$

N.B. vectors can be expanded as follows:

$$\tilde{\rho} v_r = -\Delta_H W; \quad \tilde{\rho} v_\theta = \frac{1}{r}\frac{\partial^2 W}{\partial r \partial\theta} + \frac{1}{r\sin\theta}\frac{\partial Z}{\partial\phi}; \quad \tilde{\rho} v_\phi = \frac{1}{r\sin\theta}\frac{\partial^2 W}{\partial r\partial\phi} - \frac{1}{r}\frac{\partial Z}{\partial\theta}$$

Dimensionless formulation

Reference units : MagIC

$$[d] = r_o - r_i \quad \text{(shell width)}$$

$$[t] = \frac{d^2}{\nu} \quad \text{(viscous time)}$$

$$[T] = \Delta T$$

$$[B] = \sqrt{\mu_0 \lambda \tilde{\rho} \Omega}$$

Background state (if any)

$$[\tilde{\rho}] = \tilde{\rho}(r_o) \quad ; \quad [\tilde{T}] = \tilde{T}(r_o)$$

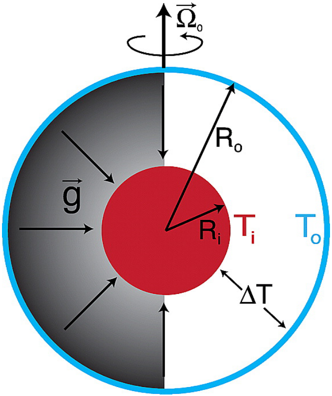

King 2010

- ν = kinematic viscosity
- $\lambda = 1/(\mu_0 \sigma)$ = magnetic diffusivity

MHD equations

Anelastic equations: LBR formulation

$$\frac{\partial \mathbf{v}}{\partial t} + (\mathbf{v}\cdot\nabla)\,\mathbf{v} = -\nabla\left(\frac{P'}{\rho_a}\right) + \frac{Ra}{Pr} g(r) S \mathbf{e}_r - \frac{2}{E}\mathbf{e}_z \times \mathbf{v} + \mathbf{F}_\nu + \frac{(\nabla\times\mathbf{B})\times\mathbf{B}}{\rho_a E Pm}$$

$$\rho_a T_a \left[\frac{\partial S}{\partial t} + (\mathbf{v}\cdot\nabla)\,S\right] = \frac{1}{Pr}\nabla\cdot(\rho_a T_a \nabla S) + \frac{Di\,Pr}{Ra}\left(Q_\nu + \frac{1}{Pm^2 E}(\nabla\times\mathbf{B})^2\right)$$

$$\nabla\cdot(\rho_a \mathbf{v}) = 0$$

$$\nabla\cdot\mathbf{B} = 0$$

$$\frac{\partial \mathbf{B}}{\partial t} = \nabla\times(\mathbf{v}\times\mathbf{B}) + \frac{1}{Pm}\nabla^2\mathbf{B}$$

with $\begin{cases} \mathbf{F}_\nu & \text{viscous force} \\ Q_\nu & \text{viscous heating} \end{cases}$

MHD equations

Boussinesq limit

$$\frac{\partial \mathbf{v}}{\partial t} + (\mathbf{v}\cdot\nabla)\mathbf{v} = -\nabla P' + \frac{Ra}{Pr} g(r) T' \mathbf{e}_r - \frac{2}{E}\mathbf{e}_z \times \mathbf{v} + \nabla^2 \mathbf{v} + \frac{1}{EPm}(\nabla\times\mathbf{B})\times\mathbf{B}$$

$$\frac{\partial T}{\partial t} + (\mathbf{v}\cdot\nabla) T = \frac{1}{Pr}\nabla^2 T$$

$$\nabla\cdot\mathbf{v} = 0$$

$$\nabla\cdot\mathbf{B} = 0$$

$$\frac{\partial \mathbf{B}}{\partial t} = \nabla\times(\mathbf{v}\times\mathbf{B}) + \frac{1}{Pm}\nabla^2\mathbf{B}$$

Boundary conditions

- Mechanical boundary conditions: no-slip or stress-free
- Thermal boundary conditions: fixed temperature or fixed flux
- Magnetic boundary conditions: vacuum, pseudo-vacuum, . . .

Control parameters

Rayleigh number $Ra = \dfrac{\alpha_o T_o g_o d^3 \Delta S}{c_p \nu \kappa}$

Ekman number $E = \dfrac{\nu}{\Omega d^2}$

Prandtl number $Pr = \nu / \kappa$

magnetic Prandtl number $Pm = \nu / \eta$

shell aspect ratio $\chi = r_\mathrm{i} / r_\mathrm{o}$

Anelastic with a polytropic reference state, $\tilde{T}$, $\tilde{\rho} = \tilde{T}^n$, $\tilde{P} = \tilde{T}^{n+1}$

density contrast $N_\rho = \ln \dfrac{\tilde{\rho}_i}{\tilde{\rho}_o}$

polytropic index n

Physical parameter regime and numerical limitations

Parameter	Earth's core	Gas giants	Sun	Simulations
E	10^{-15}	10^{-18}	10^{-15}	10^{-6}
Ra	10^{27}	10^{30}	10^{24}	10^{12}
Pr	10^{-1}	10^{-1}	10^{-6}	10^{-1}
Pm	10^{-6}	10^{-7}	10^{-3}	10^{-1}
Re	10^{9}	10^{12}	10^{13}	10^{3}

Writing the equations using the poloidal/toroidal potentials (MagIC)

- Poloidal potential: take $\mathrm{e_r}\cdot[\cdots]$ of the NS equation:

$$\mathbf{e_r}\cdot\tilde{\rho}\frac{\partial\mathbf{v}}{\partial t}=\frac{\partial}{\partial t}(\mathbf{e_r}\cdot\tilde{\rho}\mathbf{v})=-\Delta_H\frac{\partial W}{\partial t}$$

- Toroidal potential: take $\mathbf{e}_\mathrm{r}\cdot\nabla\times[\cdots]$ of the NS equation:

$$\mathbf{e_r}\cdot\boldsymbol{\nabla}\times\left(\frac{\partial\tilde{\rho}\mathbf{v}}{\partial t}\right)=\frac{\partial}{\partial t}(\mathbf{e_r}\cdot\nabla\times\tilde{\rho}\mathbf{v})=-\Delta_H\frac{\partial Z}{\partial t}$$

- Pressure: take $\nabla_H\cdot[\cdots]$ of the NS equation:

$$\nabla_H\cdot\left(\tilde{\rho}\frac{\partial v}{\partial t}\right)=\Delta_H\frac{\partial}{\partial t}\left(\frac{\partial W}{\partial r}\right)$$

N.B. Some spherical shell codes get rid of pressure by instead taking $\mathrm{e_r}\cdot\nabla\times\nabla\times[\cdots]$ to derive the equation for the toroidal potential

Deriving the different terms of NS with polo/toro potentials

One has to proceed the same way for each linear term! As an example: Coriolis force that enters the toroidal potential equation:

$$\begin{aligned}
\mathbf{e_r}\cdot\nabla\times[2\tilde{\rho}\mathbf{v}\times\mathbf{e_z}] &= 2\mathbf{e_r}\cdot[(\mathbf{e_z}\cdot\nabla)(\tilde{\rho}\mathbf{v})] \\
&= 2\left[\cos\theta\frac{\partial(\tilde{\rho}v_r)}{\partial r}-\frac{\sin\theta}{r}\frac{\partial(\tilde{\rho}v_r)}{\partial\theta}+\frac{\tilde{\rho}v_\theta\sin\theta}{r}\right] \\
&= 2\left[-\cos\theta\frac{\partial}{\partial r}(\Delta_H W)+\right. \\
&\left.\frac{\sin\theta}{r}\frac{\partial}{\partial\theta}(\Delta_H W)+\frac{\sin\theta}{r^2}\frac{\partial^2 W}{\partial r\partial\theta}+\frac{1}{r^2}\frac{\partial Z}{\partial\phi}\right]
\end{aligned}$$

PaRoDy (Boussinesq)

The toroidal component is obtained by applying the operator $\mathbf{r}\cdot\nabla\times$ to NS equation:

$$\frac{\partial}{\partial t}L_2 v_T = -\mathbf{r}\cdot\nabla\times(\mathbf{v}\cdot\nabla)\mathbf{v} + \nu L_2 \triangle v_T - 2\Omega_0 \mathbf{r}\cdot(\mathbf{e}_z\times\mathbf{v}) \tag{6}$$

Notice that the pressure gradient term and the buoyancy term have been eliminated. The Coriolis term can be rewritten as:

$$2\Omega\left((\mathbf{e}_z\times\mathbf{r})\cdot\nabla v_T - Q_3 v_P\right) \tag{7}$$

where $Q_3 = \mathbf{e}_z\cdot\nabla - \frac{1}{2}(L_2\mathbf{e}_z\cdot\nabla + \mathbf{e}_z\cdot\nabla L_2)$ (Roberts 1968). By applying $\mathbf{r}\cdot\nabla\times\nabla\times$ to NS equation:

$$\frac{\partial L_2\triangle v_P}{\partial t} = \nu\triangle L_2\triangle v_P + 2\Omega(\mathbf{e}_z\times\mathbf{r})\cdot\nabla(\triangle v_P) + 2\Omega Q_3 v_T - \alpha g L_2\Theta + \mathbf{r}\cdot\nabla\times\nabla\times(\mathbf{v}\cdot\nabla)\mathbf{v} \tag{8}$$

Nonlinear terms are calculated in physical space.

Induction and temperature equations expressed using polo/toro potentials

As derived for the equation of motion, $\mathbf{e}_r\cdot$ and $\mathbf{e}_r\cdot\nabla\times$ apply to the induction equation provide:

$$\left(\frac{\partial}{\partial t}-\lambda\triangle\right)L_2 B_P = \mathbf{r}\cdot(\nabla\times(\mathbf{v}\times\mathbf{B})) \quad (9)$$

$$\left(\frac{\partial}{\partial t}-\lambda\triangle\right)L_2 B_T = \mathbf{r}\cdot(\nabla\times(\nabla\times(\mathbf{v}\times\mathbf{B}))) \quad (10)$$

$$\frac{\partial\Theta}{\partial t} = -\frac{1}{r}\frac{dT_s}{dr}\mathbf{v}\cdot\mathbf{r}+\kappa\triangle\Theta-(\mathbf{v}\cdot\nabla)\Theta \quad (11)$$

with $\mathbf{v}\cdot\mathbf{r} = L_2 v_P/r$. and $T = T_s(r)+\Theta$.

Lignes directrices

Angular decomposition

Spherical harmonic functions Y_ℓ^m are a natural choice for the horizontal expansion in colatitude θ and longitude ϕ

$$Y_\ell^m(\theta,\phi) = P_\ell^m(\cos\theta)e^{im\phi}$$

Degree: ℓ and order: m

$$\int_0^{2\pi}\int_0^{\pi} Y_\ell^m(\theta,\phi)Y_{\ell'}^{m'*}(\theta,\phi)\sin\theta\mathrm{d}\theta\mathrm{d}\phi = \delta_{\ell\ell'}\delta^{mm'}$$

$$Y_\ell^m(\theta,\phi) = \left(\frac{(2\ell+1)}{4\pi}\frac{(\ell-|m|)!}{(\ell+|m|)!}\right)^{1/2} P_\ell^m(\cos\theta)e^{im\phi}$$

SH Representation

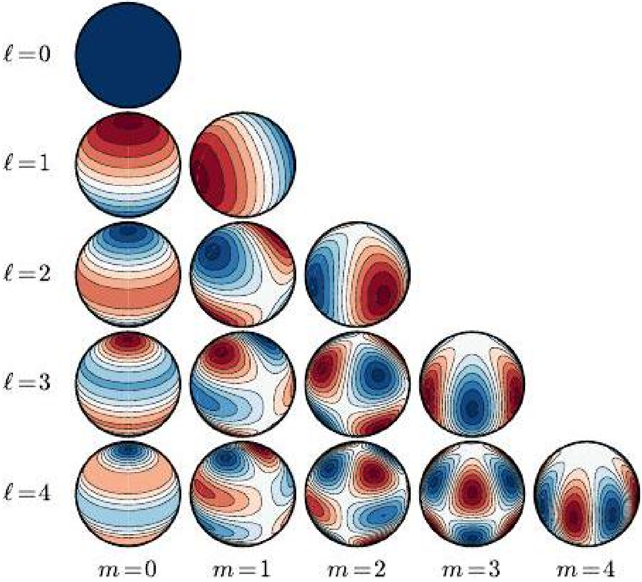

Some mathematical properties of the spherical harmonics (SH)

- Complete and orthogonal eigenfunctions of Δ_H (or L_2):

$$\Delta_H Y_\ell^m = -\frac{\ell(\ell+1)}{r^2} Y_\ell^m \qquad L_2 Y_l^m = l(l+1) Y_l^m$$

- Some useful recursion relations:

$$\cos\theta\, Y_\ell^m = c_{\ell+1}^m Y_{\ell+1}^m + c_\ell^m Y_{\ell-1}^m$$
$$\sin\theta \frac{\partial Y_\ell^m}{\partial\theta} = \ell c_{\ell+1}^m Y_{\ell+1}^m - (\ell+1) c_\ell^m Y_{\ell-1}^m$$
$$\text{with} \quad c_{\ell m} = \left[\frac{(\ell+m)(\ell-m)}{(2\ell+1)(2\ell-1)}\right]^{1/2}$$

- Practically this is how θ and ϕ derivatives are computed in MagIC and *PaRoDy*.

From spatial to spectral space

$$(r,\theta,\phi) \rightarrow (r,\ell,m)$$

Suppose we have $Z(r,\theta,\phi,t)$ on a longitude/latitude representation $\left(N_\theta, N_\phi\right)$. The expansion of the horizontal structure in series of SH yields:

$$Z(r,\theta,\phi,t) = \sum_{\ell=0}^{\ell_{\max}} \sum_{m=-\ell}^{\ell} Z_\ell^m(r,t) Y_\ell^m(\theta,\phi)$$

SH representation truncated at degree $\ell_{\max}$ and order $m_{\max}$.

MHD equations in *PaRoDy*

$$\frac{\partial}{\partial t}\Delta v_{p_l}^m = \nu \Delta^2 v_{p_l}^m + i2\Omega \frac{m}{l(l+1)} \Delta v_{p_l}^m + 2\Omega \frac{1}{l(l+1)} Q_3 v_{t_l}^m$$

$$- \alpha g(r) \Theta_l^m$$

$$+ \frac{1}{l(l+1)} \vec{r} \cdot \vec{\nabla} \wedge \left(\vec{\nabla} \wedge \left(\vec{v} \nabla \vec{v} - \frac{1}{\mu_0 \rho_0} \vec{B} \nabla \vec{B} \right) \right) \Big|_{Y_l^m}$$

$$\frac{\partial}{\partial t} v_{tl}^m = \nu \Delta v_{tl}^m + i2\Omega \frac{m}{l(l+1)} v_{tl}^m - 2\Omega \frac{1}{l(l+1)} Q_3 v_{p_l}^m$$

$$- \frac{1}{l(l+1)} \vec{r} \cdot \left(\vec{\nabla} \wedge \left(\vec{u} \underline{\nabla} \vec{v} - \frac{1}{\mu_0 \rho_0} \vec{B} \nabla \vec{B} \right) \right) \Big|_{Y_l^m}$$

$$\frac{\partial}{\partial t} \Theta_l^m = - \left(\frac{1}{r} \frac{\partial T_s}{\partial r} \right) l(l+1) v_{pl}^m + \kappa \Delta \Theta_l^m - (\vec{v} \cdot \vec{\nabla} \Theta) \Big|_{Y_l^m}$$

$$\frac{\partial}{\partial t} B_{Pl}^m = \lambda \Delta B_{Pl}^m + \frac{1}{l(l+1)} \vec{r} \cdot (\vec{\nabla} \wedge (\vec{v} \wedge \vec{B})) \Big|_{Y_l^m}$$

$$\frac{\partial}{\partial t} B_{Tl}^m = \lambda \Delta B_{Tl}^m + \frac{1}{l(l+1)} \vec{r} \cdot (\vec{\nabla} \wedge (\vec{\nabla} \wedge (\vec{v} \wedge \vec{B}))) \Big|_{Y_l^m}$$

Application:

As an example, let us focus on the derivation of the equation for the poloidal magnetic field potential:

$$\frac{\partial \mathbf{B}}{\partial t} = \nabla \times (\mathbf{v} \times \mathbf{B}) + \frac{1}{Pm} \Delta \mathbf{B}$$

To derive the equation for $B_{P\ell}^m$, take the radial component of the induction equation:

$$\mathbf{e_r} \cdot \frac{\partial \mathbf{B}}{\partial t} = \frac{\partial B_r}{\partial t} \qquad \text{Time derivative}$$

$$B_r(r,\theta,\phi,t) = -\Delta_H B_P = \sum_{\ell,m} \frac{\ell(\ell+1)}{r^2} B_{P\ell}^m(r,t) Y_\ell^m(\theta,\phi)$$

Hence

$$\mathbf{e_r} \cdot \frac{\partial \mathbf{B}}{\partial t} = \sum_{\ell,m} \frac{\ell(\ell+1)}{r^2} \frac{\partial B_{P\ell}^m}{\partial t} Y_\ell^m$$

Application: the diffusion term

$$\mathbf{e_r} \cdot \left(\frac{1}{Pm} \Delta \mathbf{B} \right) = \frac{1}{Pm} \left(\Delta B_r - \frac{2}{r^2} B_r - \frac{2}{r} \nabla_H \cdot \mathbf{B} \right)$$

$$= \frac{1}{Pm} (\Delta B_r - \frac{2}{r^2} B_r - \underbrace{\boldsymbol{\nabla} \cdot \mathbf{B}}_{=0} + \frac{2}{r^3} \frac{\partial}{\partial r} \left(r^2 B_r \right))$$

$$= \frac{1}{Pm} \left(\frac{1}{r^2} \frac{\partial^2 \left(r^2 B_r \right)}{\partial r^2} + \Delta_H B_r \right)$$

Hence

$$\mathbf{e_r} \cdot \left(\frac{1}{Pm} \Delta \mathbf{B} \right) = \frac{1}{Pm} \sum_{\ell,m} \frac{\ell(\ell+1)}{r^2} \left(\frac{\partial^2 B_{P\ell}^m}{\partial r^2} - \frac{\ell(\ell+1)}{r^2} B_{P\ell}^m \right) Y_\ell^m$$

Lignes directrices

1. Introduction
2. Science with *PaRoDy* or MagIC
   - 3D MHD Spherical Couette Flow: Tayler-Spruit dynamo
   - MRI in rapidly rotating spherical shells
   - Convective dynamos
   - Coriolis effects in hydro anelastic models
   - Magnetic effects
3. **Numerical methods**
   - The poloidal/toroidal decomposition
   - Angular decomposition: Spherical Harmonics (SH)
   - **Rdial discretization**
   - Time integration
   - Resolution cheks

Radial representation: different strategies

- calypso, *PaRoDy*, Xshells. . . : finite differences (usually 2nd order).
- ASH, Rayleigh. . . : expansion in Chebyshev polynomials.
- MagIC: since version 5.6: both finite differences and Chebyshev polynomials are supported.

Finite differences are cheaper: sparse matrix, less memory, faster inversion and enable a simple strategy for parallelization. . .

Finite Differences

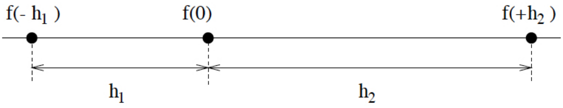

Second order scheme:

$$(\delta f)_0 = \frac{f(h) - f(-h)}{2h}$$

$$\left(\delta^2 f\right)_0 = \frac{f(-h) - 2f(0) + f(h)}{h^2}$$

$$\frac{\partial f}{\partial x}(0) = (\delta f)_0 + \tau_0$$

$$\tau_0 = -\frac{h^2}{6}\frac{\partial^3 f}{\partial x^3}(0) - \frac{h^4}{120}\frac{\partial^5 f}{\partial x^5}(0) + \mathcal{O}\left(h^6\right)$$

$$\frac{\partial^2 f}{\partial x^2}(0) = \left(\delta^2 f\right)_0 + \tau_0'$$

$$\tau_0' = -\frac{h^2}{12}\frac{\partial^4 f}{\partial x^4}(0) - \frac{h^4}{360}\frac{\partial^6 f}{\partial x^6}(0) + \mathcal{O}\left(h^6\right)$$

Finite Differences

First order scheme:

$$(\tilde{\delta} f)_0 = \frac{h_1}{h_1+h_2}\left(\frac{f(h_2)-f(0)}{h_2}\right) + \frac{h_2}{h_1+h_2}\left(\frac{f(0)-f(-h_1)}{h_1}\right)$$

$$\frac{\partial f}{\partial x}(0) = (\tilde{\delta} f)_0 + \tilde{\tau}_0$$

$$\tilde{\tau}_0 = -\frac{h_1 h_2}{6}\frac{\partial^3 f}{\partial x^3}(0) + \mathcal{O}\left(h^3\right),$$

$$\left(\tilde{\delta}^2 f\right)_0 = \frac{\tilde{\delta} f\left(\frac{h_2}{2}\right) - \tilde{\delta} f\left(-\frac{h_1}{2}\right)}{(h_1+h_2)/2}$$

$$\left(\tilde{\delta}^2 f\right)_0 = \frac{h_2 f(-h_1) - (h_1+h_2) f(0) + h_1 f(h_2)}{(h_1 h_2 (h_1+h_2))/2}.$$

Lignes directrices

Time integration and the diffusive terms

This analytical solution can be compared to a solution resulting from a numerical method in order to better understand their efficiency. Consider an explicit scheme:

$$\frac{B_j^{n+1} - B_j}{\delta t} = \lambda \left(\frac{B_{j+1}^n - 2B_j^n + B_{j-1}^n}{\delta x^2} \right) \qquad B_j^n = B(x_j, t_n) \tag{12}$$

A Von Neuman analysis provides the stability condition for this scheme:

$$\frac{\lambda \delta t}{\delta x^2} \leq \frac{1}{2} \tag{13}$$

The stability of this scheme can be improved by considering a combination of explicit and implicit terms. This scheme is the Crank-Nicholson one:

$$\frac{B_j^{n+1} - B_j}{\delta t} = \lambda \left(\frac{1}{2} \frac{B_{j+1}^n - 2B_j^n + B_{j-1}^n}{\delta x^2} \right) \tag{14}$$

$$\lambda \left(\frac{1}{2} \frac{B_{j+1}^{n+1} - 2B_j^{n+1} + B_{j-1}^{n+1}}{\delta x^2} \right) \tag{15}$$

Radial representation and time integration

$$\frac{\partial}{\partial t}\Delta v_{Pl}^m = \nu\Delta^2 v_{Pl}^m + \mathrm{i}2\Omega\frac{m}{l(l+1)}\Delta v_{Pl}^m + 2\Omega\frac{1}{l(l+1)}Q_3 v_{Tl}^m$$
$$- \alpha g(r)\Theta_\ell^m + \frac{1}{l(l+1)}\vec{r}\cdot\vec{\nabla}\wedge\left(\vec{\nabla}\wedge\left(\vec{v}\nabla\vec{v} - \frac{1}{\mu_0\rho_0}\vec{B}\nabla\mathbf{B}\right)\right)\Bigg|_{Y_\ell^m}$$

Laplacian and bi-Laplacian become sparse matrices (tri-diagonal, 5-bands) by using finite differences for the radial derivatives. At each timestep, they must be inverted (semi-implicit scheme).

$$\left(-\frac{\lambda}{2\delta x^2}, \frac{1}{\delta t} + \frac{\lambda}{\delta x^2}, -\frac{\lambda}{2\delta x^2}\right)\cdot\begin{pmatrix} B_{j+1}^{n+1} \\ B_j^{n+1} \\ B_{j-1}^{n+1} \end{pmatrix} = \left(\frac{\lambda}{2\delta x^2}, \frac{1}{\delta t} - \frac{\lambda}{\delta x^2}, \frac{\lambda}{2\delta x^2}\right)\cdot\begin{pmatrix} B_{j+1}^{n} \\ B_j^{n} \\ B_{j-1}^{n} \end{pmatrix}$$

The matrices are constant except when the timestep changes.

Time integration

Generic evolution equation with terms $\mathcal{I}(v,t)$ to be treated implicitly and $\mathcal{E}(v,t)$ to be treated explicitly:

$$\frac{\partial \mathbf{v}}{\partial t} + \overbrace{\mathcal{I}(\mathbf{v},t)}^{\Delta \mathbf{v}} = \underbrace{\mathcal{E}(\mathbf{v},t)}_{\text{nonlinear, Coriolis terms...}}$$

Glatzmaier's (1984) time integration scheme (2nd order): semi-Implicit Crank-Nicolson scheme:

$$\left(\frac{v(t+\delta t)-v(t)}{\delta t}\right)_{\mathcal{I}} = -\alpha\mathcal{I}(v,t+\delta t)-(1-\alpha)\mathcal{I}(v,t)$$

Explicit 2nd order Adams-Bashforth scheme:

$$\left(\frac{v(t+\delta t)-v(t)}{\delta t}\right) = \frac{3}{2}\mathcal{E}(v,t)-\frac{1}{2}\mathcal{E}(v,t-\delta t)$$

Adaptative timestep: Courant condition

- Explicit treatment of the Coriolis force: $\delta t \leq 0.1 E$ (MagIC)
- δt should be smaller than the advection between two grid points:

$$\delta t \leq \min\left[\frac{\delta r}{|v_r|}\right]; \delta t \leq \min\left[\left(\frac{r^2}{\ell_{\max}(\ell_{\max}+1)\left(v_\theta^2+u_\phi^2\right)}\right)^{1/2}\right]$$

- In presence of a magnetic field, another condition on the Alfvèn velocity is required.

Hybrid (MPI/OpenPM) configuration used in MagIC and *PaRoDy*

MPI:

1st part of the code: radial levels can be treated independently: r is distributed over N_p MPI ranks.
2nd part of the code (MagIC): time advance of the equations = linear solve = all the $(\ell; m)$ modes can be treated independently: $(\ell; m)$ is distributed over N_p MPI ranks (pairing needed to ensure the load balancing

OpenMP:

1st part of the code: N_t OpenMP threads can be used over the blocks for the SH transforms and computation of nonlinear terms (SHTns library).

Lignes directrices

Resolution checks: visualisation

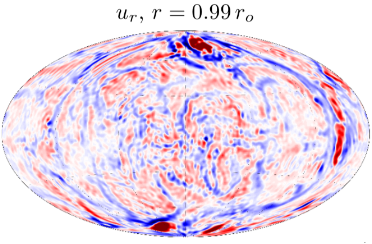

Resolution checks: spectra

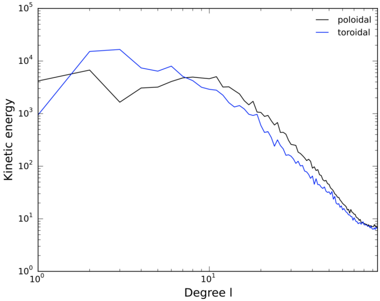

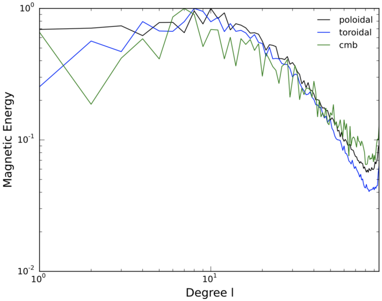

Resolution checks

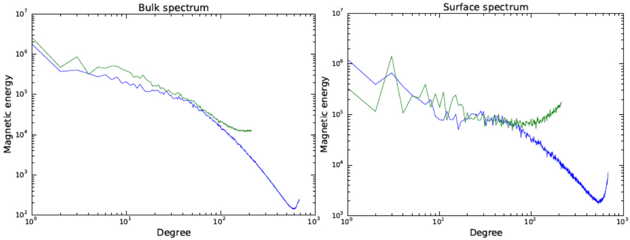

- At first glance, you would better trash the under-resolved case
- **But, the largest scales contributions are reasonably captured**
- Surprisingly, some **global quantities** might still be OK!